Rapid Deposition of Gold Nanoparticle Films with Controlled Thickness and Structure by Convective Assembly

Brian G. Prevo,[†] Joseph C. Fuller, III,[‡] and Orlin D. Velev*,[†]

Department of Chemical and Biomolecular Engineering, North Carolina State University, Raleigh, North Carolina 27695-7905, and Department of Chemical Engineering, Lehigh University, Bethlehem, Pennsylvania 18015

We report how convective assembly at high volume fraction combined with thermal treatment allows robust fabrication of gold nanocoatings whose structure can be varied and correlated to their optical properties and conductance. Uniform films of gold nanoparticles were deposited directly from aqueous suspensions, where neither the nanoparticles, nor the substrates, were covered with ligands or pretreated in any way. The number of layers, optical absorbance, and electrical conductance of these nanocoatings could be controlled by the speed of deposition. The electronic, optical, and structural properties of the nanoparticle multilayers could be further tuned by post-deposition heat treatment. Scanning electron microscopy observations and electrical conductance measurements showed that heating leads to a transition from a near-percolated nanoparticle structure (conductivity approaching 2000 $\Omega^{-1}cm^{-1}$) to a discontinuous insular structure (conductivity $<10^{-5}$ $\Omega^{-1}cm^{-1}$). These structural transitions change the coating transmission spectra, where the surface plasmon resonance peak could be tuned by heating to any value from 800 to 565 nm. The ability to tune the nanocoating structure and spectral and electronic properties may allow for applications such as nonohmic switching, quantum electronics and sensors.

Introduction

Metallic nanoparticles possess unique size-dependent properties due to their enormous surface-to-volume ratio, electron plasmon resonance, and quantum confinement effects. Thin films of such nanoparticles could be used in applications such as reflective coatings, sensors,[1−3] platforms for molecular electronics and plasmonics,[1−3] substrates for surface-enhanced Raman spectroscopy,[4] and materials with high catalytic activity and specificity.[5,6] Two main approaches have been used for making metallic films from nanoparticles: (1) top-down via deposition of evaporated or sputtered metal from vacuum to a substrate[7,8] or to a polymer matrix,[9] or (2) bottom-up via "soft" lithography stamping,[10] self-assembly of sterically protected nanoparticles,[11,12] sol−gel coating,[13,14] or adsorption of nanoparticles onto oppositely

charged substrates.[15,16] Approaches (1) and (2) can be combined to make dispersed metal island films.[17] These techniques have been much investigated,[18] but are relatively complicated and inflexible. Vacuum metal deposition requires high energy input and high cleanliness. The self-assembly methods deposit one layer at a time and to date use either particles that are chemically modified (typically by coating with an organic ligand to prevent aggregation) or chemically functionalized substrates to adsorb the particles. Multiple layers can be made via layer by layer adsorption, but this requires covering of the particles and the substrates with polyelectrolytes, multiple steps, and results in organic−metallic composites.

We demonstrate how multilayer coatings from gold nanoparticles can be fabricated in one step by convective assembly from an evaporating meniscus of aqueous suspension. The convective assembly has been shown to be a simple and facile route for deposition of two-dimensional crystals from polystyrene latex and silica microspheres.[19−22] The method can also be applied for making coatings from

---

* Corresponding author. E-mail: odvelev@unity.ncsu.edu.
[†] North Carolina State University.
[‡] Lehigh University.

(1) Shipway, A. N.; Katz, E.; Willner, I. *Chemphyschem* **2000**, *1*, 18−52.
(2) Brust, M.; Kiely, C. J. *Colloid Surf. A* **2002**, *202*, 175−186.
(3) Convertino, A.; Capobianchi, A.; Valentini, A.; Cirillo, E. N. M. *Adv. Mater.* **2003**, *15*, 1103−1107.
(4) Tessier, P. M.; Christensen, S. D.; Ong, K. K.; Clemente, E. M.; Lenhoff, A. M.; Kaler, E. W.; Velev, O. D. *Appl. Spectrosc.* **2002**, *56*, 1524−1530.
(5) Dai, J. H.; Bruening, M. L. *Nano Lett.* **2002**, *2*, 497−501.
(6) Sun, L.; Crooks, R. M. *Langmuir* **2002**, *18*, 8231−8236.
(7) Tour, J. M.; Cheng, L.; Nackashi, D. P.; Yao, Y. X.; Flatt, A. K.; St Angelo, S. K.; Mallouk, T. E.; Franzon, P. D. *J. Am. Chem. Soc.* **2003**, *125*, 13279−13283.
(8) Meriaudeau, F.; Downey, T. R.; Passian, A.; Wig, A.; Ferrell, T. L. *Appl. Opt.* **1998**, *37*, 8030−8037.
(9) Heilmann, A. *Polymer Films with Embedded Metal Nanoparticles*; Springer: New York, 2003.
(10) Ng, W. K.; Wu, L.; Moran, P. M. *Appl. Phys. Lett.* **2002**, *81*, 3097−3099.

(11) Brust, M.; Bethell, D.; Schiffrin, D. J.; Kiely, C. J. *Adv. Mater.* **1995**, *7*, 795.
(12) Korgel, B. A.; Fitzmaurice, D. *Phys. Rev. Lett.* **1998**, *80*, 3531−3534.
(13) Kozuka, H.; Sakka, S. *Chem. Mater.* **1993**, *5*, 222−228.
(14) Selvan, S. T.; Hayakawa, T.; Nogami, M.; Kobayashi, Y.; Liz-Marzan, L. M.; Hamanaka, Y.; Nakamura, A. *J. Phys. Chem. B* **2002**, *106*, 10157−10162.
(15) Decher, G.; Eckle, M.; Schmitt, J.; Struth, B. *Curr. Opin. Colloid Interface Sci.* **1998**, *3*, 32−39.
(16) Musick, M. D.; Keating, C. D.; Lyon, L. A.; Botsko, S. L.; Pena, D. J.; Holliway, W. D.; McEvoy, T. M.; Richardson, J. N.; Natan, M. J. *Chem. Mater.* **2000**, *12*, 2869−2881.
(17) Whitney, A. V.; Myers, B. D.; Van Duyne, R. P. *Nano Lett.* **2004**, *4* (8), 1507−1511..
(18) Fendler, J. H. *Chem. Mater.* **2001**, *13*, 3196−3210.

Convective Assembly Deposition of Gold Nanofilms

Chem. Mater., Vol. 17, No. 1, 2005 29

sterically protected,[23] or silica-encapsulated[24] nanoparticles. Similar mesoscopically ordered films can be deposited from surfactant-stabilized nanoparticles dispersed within silica sols.[25] Convective assembly of films from "naked" (chemically unprotected) metallic nanoparticles on unfunctionalized substrates requires preparing concentrated nanoparticle suspensions, which had been difficult because of the propensity of unprotected metal nanoparticles to aggregate upon concentration due to van der Waals attraction. We developed procedures for nanoparticle concentration by membrane filtration (via centrifugation), and an apparatus for convective assembly at high volume fractions that allows efficient deposition of nanoparticle coatings from droplet-sized volumes of suspension.[26] The combination of these two techniques allowed controlled efficient assembly of a wide variety of structures from as-synthesized gold nanoparticles without any functionalization of the substrates. The first systematic data on the structure, optical, and electronic properties of such multilayer nanocoatings are reported here. We show how the properties of these coatings can be correlated to their structure, and modified in a wide range via controllable fusion at temperatures much below the melting point of the bulk metal.

The unusual optical and electrical properties of the thin metal nanoparticle films are a strong function of the size, shape, and proximity of the particles.[9,27] Dispersed or unaggregated particles exhibit surface plasmon resonance (SPR) absorption bands due to free electron oscillation at a specific frequency of incident light.[28] The structure of a thin film of separated nanoparticles can be approximated by homogeneously distributed spheres, and their spectral characteristics can be modeled by effective medium approximations such as the Maxwell−Garnett theory.[24] Particle aggregation, however, leads to multipolar electronic interactions, and increasingly complex effective media approximations are required to model the coating optical properties.[9,29] Larger domains exhibit increasingly broad absorbance peaks at progressively longer wavelengths (red shifted) and are marked by a macroscopic change in coloration from reddish to bluish.[30] When the aggregated metallic domains exceed several hundred nanometers bulk metallic properties are observed. Microscopy techniques including SEM, SPM, and TEM have been used to provide microstructural information required for improved model accuracy in the effective media theories.[9]

The electrical conductivity of metal nanocoatings can vary over many orders of magnitude ranging from metallic at very high particle filling fractions (conductivity $\sim 10^5$ to 10^6 Ω^{-1} cm^{-1}), to insulating (conductivity $\sim 10^{-14}$ to 10^{-16} Ω^{-1}cm^{-1}) at low filling fractions.[9] Near the percolation threshold (filling fraction of ~ 0.5 for most metals), a sharp transition between metallic and insulating behavior occurs.[9] In thin metallic films of this type, nonohmic "switching" between low and high conductivities has been widely reported,[9,11,31] and studies have shown that this phenomenon can be reversible and cyclic.[7] The switching phenomenon occurs at threshold voltages that overcome the energy barrier to conduction between metal−insulator−metal regions. Such a process has been described as "self-forming" conduction pathways.[32,33] The sensitivity of these conductivity changes to adsorbed or deposited organics has potential for making gas-phase chemical sensors.[23,34,35]

Nanoparticle metallic films are also sensitive to temperature treatment due to the melting point depression (MPD) inherent to small particles.[9,31] MPD becomes significant for sub-100-nm particles.[36−38] It is dependent on the inverse particle diameter, $1/d$, and can be well approximated by a Taylor series expansion of the Kelvin equation.[39−42] The melting point decreases rapidly for $d < 30$ nm, and shape anisotropy and even moderate size polydispersities of $\pm 10\%$ can cause large broadening of the observed melting point.[40] For low to moderate temperatures, the electrical conductivities of metal nanocoatings have shown an Arrhenius dependence on temperature.[23] At temperatures approaching the depressed melting point, however, the conductivities decrease sharply and the films become insular due to structural changes. Such sensitivity to temperatures suggests that discontinuous metallic coatings of well-controlled particle sizes could be used as temperature-sensitive thin film fuses.[31]

Experimental Section

Materials. The aqueous suspensions of gold nanoparticles were synthesized by the reduction of HAuCl$_4$ using sodium citrate (all chemicals from Aldrich, Milwaukee, WI) and were subsequently concentrated via centrifugation using Millipore Biomax 5 filters following the procedures described earlier.[26] Transmission electron microscopy was used to determine an average particle diameter of 16.3 ± 3 nm from a statistical population of over 100 particles (Figure 1), which was in good agreement with the observed UV/ vis plasmon resonance band at 522 nm. The substrates for the

(19) Dimitrov, A. S.; Nagayama, K. *Chem. Phys. Lett.* **1995**, *243*, 462−468.
(20) Jiang, P.; Bertone, J. F.; Hwang, K. S.; Colvin, V. L. *Chem. Mater.* **1999**, *11*, 2132−2140.
(21) Denkov, N. D.; Velev, O. D.; Kralchevsky, P. A.; Ivanov, I. B.; Yoshimura, H.; Nagayama, K. *Langmuir* **1992**, *8*, 3183−3190.
(22) Dimitrov, A. S.; Miwa, T.; Nagayama, K. *Langmuir* **1999**, *15*, 5257−5264.
(23) Brust, M.; Bethell, D.; Kiely, C. J.; Schiffrin, D. J. *Langmuir* **1998**, *14*, 5425−5429.
(24) Ung, T.; Liz-Marzan, L. M.; Mulvaney, P. *Colloid Surf. A* **2002**, *202*, 119−126.
(25) Fan, H. Y.; Yang, K.; Boye, D. M.; Sigmon, T.; Malloy, K. J.; Xu, H. F.; Lopez, G. P.; Brinker, C. J. *Science* **2004**, *304*, 567−571.
(26) Prevo, B. G.; Velev, O. D. *Langmuir* **2004**, *20*, 2099−2107.
(27) Blatchford, C. G.; Campbell, J. R.; Creighton, J. A. *Surf. Sci.* **1982**, *120*, 435−455.
(28) Kelly, K. L.; Coronado, E.; Zhao, L. L.; Schatz, G. C. *J. Phys. Chem. B* **2003**, *107*, 668−677.
(29) Dalacu, D.; Martinu, L. *J. Opt. Soc. Am. B* **2001**, *18*, 85−92.
(30) Turkevich, J. *Gold Bull.* **1985**, *18*, 125−131.
(31) Morris, J. E.; Coutts, T. J. *Thin Solid Films* **1977**, *47*, 3−65.
(32) Pagnia, H.; Sotnik, N. *Physica A* **1988**, *108*, 11−65.
(33) Blessing, R.; Pagnia, H. *Thin Solid Films* **1978**, *52*, 333−341.
(34) Shipway, A. N.; Lahav, M.; Willner, I. *Adv. Mater.* **2000**, *12*, 993−998.
(35) Morris, J. E. *Vacuum* **1998**, *50*, 107−113
(36) Castro, T.; Reifenberger, R.; Choi, E.; Andres, R. P. *Phys. Rev. B* **1990**, *42*, 8548−8556.
(37) Heilmann, A.; Werner, J. *Thin Solid Films* **1998**, *317*, 21−26.
(38) Pashley, D. W. *Adv. Phys.* **1965**, *14*, 327.
(39) Buffat, P.; Borel, J. P. *Phys. Rev. A* **1976**, *13*, 2287−2298.
(40) Dick, K.; Dhanasekaran, T.; Zhang, Z. Y.; Meisel, D. *J. Am. Chem. Soc.* **2002**, *124*, 2312−2317.
(41) Borel, J. P. *Surf. Sci.* **1981**, *106*, 1−9.
(42) Xue, Y. Q.; Zhao, Q. S.; Luan, C. H. *J. Colloid Interface Sci.* **2001**, *243*, 388−390.
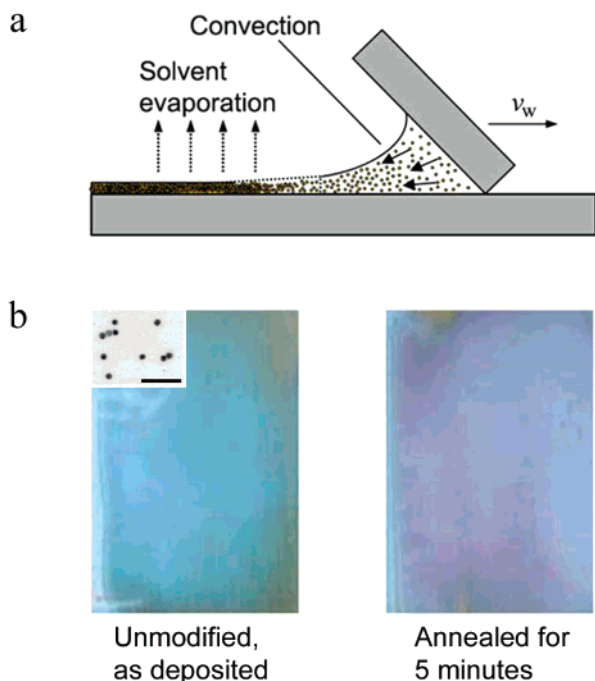
a

b

Figure 1. (a) Schematic of multilayer nanoparticle coating via convective assembly. (b) Images of actual nanocoatings deposited at 5.3 μm/s on glass prior to and after flame annealing (each image shows an area of 2.5 × 1.7 cm^2); the upper left inset is a TEM micrograph of the as-synthesized gold hydrosol particles (scale bar = 100 nm).

nanocoatings were either glass microscope slides (frosted, from Fisher Scientific, PA) or polystyrene (PS) microscope slides (sterile PS, EMS, Washington, PA; T_g ~105 °C, T_M ~230 °C). The glass slides were cleaned and hydrophilized by immersion in Nochromix (Godax Labs).[26] The PS slides were used as purchased, but 0.1– 0.2 wt % of nonionic surfactant (Tween 20 obtained from Acros Organics, NJ) was added to the water suspensions to facilitate PS wetting.

Nanoparticle Deposition. The setup and the process for deposition by convective assembly at high volume fraction were described previously.[26] Droplets (10–30 μL) of preconcentrated gold nanoparticles (2–3 wt %) dispersed in water were injected into the wedge between a substrate slide and a coating slide meeting at an angle of 23°. The droplet was held in the wedge between the surfaces by capillarity. When the top slide was translated across the substrate, a thin wetting film was formed as the meniscus stretched behind the moving slide. The evaporation of the water from within the thin wetting film is the driving force for the convective assembly of the particles comprising the coating (Figure 1a). The surface coverage of the nanoparticles is conveniently controlled by the deposition speed[26] and ranged from less than a complete monolayer to uniform multilayers.

Postdeposition Annealing. Simultaneous tuning of the structure, optical spectra, and electronic conductivity of the films was performed by gradual fusion of the particles upon heating at temperatures of 50–400 °C, well below the bulk melting temperature of gold (1064 °C). Coatings were reproducibly flash-heated by flaming (glass substrates only) or microwaving ranging from 10 s to 10 min. Flame-heating was performed by positioning the sample horizontally (gold side up) 12 cm above a Bunsen burner. The gas flow and air inlet were adjusted so that the top of the flame was just beneath the underside of the glass substrate. Other samples were exposed to microwave irradiation in a General Electric 1100 W microwave oven (2.45 GHz magnetron source). The heat released by microwave radiation is concentrated in the metal film because of its high attenuation by metals versus near complete

transmission by amorphous polymers and glasses.[43] Microwave radiation has been used for localized heating in metallic and inorganic materials.[44,45] A Raytek Raynger ST contactless infrared thermal probe (Santa Cruz, CA) was used to measure the temperature of the coatings during heating. These flash-heating techniques were proven reproducible and were commensurate with the innate simplicity and speed of the film deposition.

Characterization. The optical properties of the coatings were characterized by ultraviolet (UV)/visible (vis) absorbance spectrophotometry (Jasco V550). A custom plate holder was used and the substrate backgrounds were subtracted using a reference beam. The microstructure of the films was observed by SEM (JEOL 6400F operating at 4–5 kV). The electrical conductance of the films was measured by connecting the sample to a direct current (DC) circuit via a two-point probe. Conductive copper tape (3M, St. Paul, MN) was placed at the edges of the coating to which "alligator" clips were attached. The current–voltage, $I(V)$, response was recorded while incrementally varying the applied DC voltage between 0 and 12 V. The resistance, R, was calculated by linear regression of the $I(V)$ data.[46]

Changes in nanocoating adhesion due to heating were investigated using a custom-made "scratch" test setup. A 3-mm copper sphere was attached to a slip of flexible plastic sheet. The combined weight was recorded, and then it was attached to the deposition device and dragged across the gold nanoparticle coatings at a constant speed of 100 μm/s. The normal weight of the sphere (3 mN) provided the scratching force as it was translated laterally across the coatings. The use of the comparatively large stylus (the copper sphere) distributed the scratching force so that a lower surface pressure was exerted (compared to the fine styluses used commercially) and allowed resolution of the subtle annealing effects. Scratch testing was performed at ambient conditions, after the coatings had cooled. Substrate surfaces were assumed to be uniform in all cases. The scratch widths were measured using optical microscopy (Olympus BX 61) and a CCD camera (Olympus DP 70).

Results and Discussion

Effect of Deposition Speed. Nanocoatings with different thicknesses were deposited from the concentrated gold nanoparticle suspension by varying the meniscus withdrawal velocity v_w. As we have demonstrated earlier, v_w allows convenient and easy control of the film thickness in convective assembly.[26] All gold nanoparticle coatings had the characteristic yellow "golden" appearance when viewed in reflected light. They were also semi-transparent and their appearance in transmitted light ranged from blue tinted, for thin, rapidly deposited films, to darker blue/gold coloration, for thicker, more slowly deposited coatings (Figure 1b). The interrelation between coating deposition speed and the measured UV/vis absorbance spectra is shown in Figure 2a. Qualitatively, the spectra for unmodified coatings were the same, save that the absorbance (or optical density) increased

(43) Liao, S. Y. *IEEE Trans. Microwave Theory Tech.* **1975**, *23*, 846– 849.
(44) Rao, K. J.; Vaidhyanathan, B.; Ganguli, M.; Ramakrishnan, P. A. *Chem. Mater.* **1999**, *11*, 882–895.
(45) Ren, T. Z.; Yuan, Z. Y.; Su, B. L. *Langmuir* **2004**, *20*, 1531–1534.
(46) The measured resistance, R_M, is a sum of three resistors in series— two copper tape leads and the coating sample itself. In every case the independently measured resistance of the copper tape and connecting leads, $R_{Cu} = 0.001$ Ω, was such that $R_{Cu} \ll R_M$ and thus, the resistance of the coating sample, R_S, was effectively equivalent to the measured resistance, $R_S = R_M$.
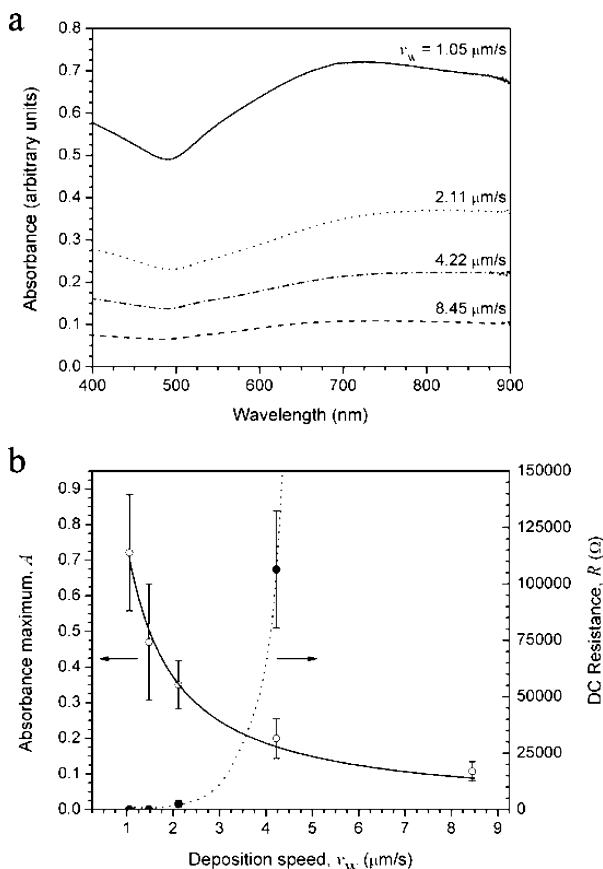
Figure 2. (a) Absorbance spectra of gold nanocoatings on glass deposited at different deposition speeds, v_w (all other deposition parameters being constant). (b) Absorbance maximum, A, (open circles) and DC electrical resistance, R, (solid circles) of the same samples plotted as a function of deposition speed. Solid line is a least-squares fit to $A = k/v_w$. The dotted line through the resistance data is to guide the eye.

with decreasing deposition speed, proving that slower speeds yield thicker coatings of aggregated gold nanoparticles.[23,47] Within experimental error the absorbance maximum, A, was inversely proportional to the deposition speed, $A \approx 1/v_w$ (Figure 2b). A single fitting parameter of 0.74 obtained by the least-squares method was used to generate the curve in Figure 2b. The $A \approx 1/v_w$ dependence is in good agreement with our previously reported observations that the surface coverage measured via optical microscopy scaled inversely with deposition speed, v_w.[26]

Spectrophotometry of the red-colored gold sols prior to deposition showed the characteristic SPR peak at ~520 nm indicative of stable dispersions of 10−20 nm particles. The peak in the absorbance spectra of the as-deposited nanoparticle films (Figure 2a) was strongly red shifted to about 750−850 nm and quite broad compared to the SPR peak for gold nanoparticle dispersions. This large shift indicates that the coatings are comprised of large domains of highly aggregated particles, which provide an effectively infinite conduction path to the free electrons (similarly to bulk metal). The gold coatings deposited on PS substrates followed the same behavior, but their initial average SPR wavelength was ~700 nm, or slightly smaller than that for glass-based coatings. This blue shift for PS-based coatings implies a

reduced degree of aggregation, which may be attributed to the stabilizing effect of the dilute surfactant used to improve the wetting of the polymer substrate.

The electronic properties of the self-assembled films also depended strongly on the deposition speed (Figure 2b). At speeds $v_w \le 2$ μm/s the coatings were very conductive and showed little dependence on the rate of deposition. The resistances of these coatings were ~50 Ω ($R = 45 \pm 16$ Ω for coatings deposited at 1.05 μm/s and $R = 54 \pm 17$ Ω for those deposited at 1.48 μm/s). The uniform films deposited at such slow speeds were of typical dimensions 0.5 cm long (l), 2.5 cm wide (w), and approximately 400 nm thick (t). The average coating conductivity,[48] $\sigma = l/(Rtw)$, is thus estimated to be 2000 Ω^{-1} cm^{-1}. These data are comparable to literature values for semi-continuous metallic films of intermediately high coverage fractions, $f > 0.5$, made from either co-sputtered metal/polymer composites or evaporated metal on polymer films, which exhibit conductivities in the range of 0.01−100 Ω^{-1} cm^{-1}.[9] The reduced conductivity of such discontinuous metallic films compared to that of bulk gold (4.26 × 10^5 Ω^{-1} cm^{-1})[48] can be attributed to their high porosity, and small constitutive particle size which results in electron mean free path limitation due to electron reflection at nanoparticle/insulator barriers and intraparticle grain boundaries.[9,49]

Coatings deposited at fast deposition speeds ($v_w \ge 8.45$ μm/s) were effectively insulating, as the resistance of the films was so high that the meter did not register any current: $R_S > 2 \times 10^9$ Ω. This result correlates with the low spectrophotometric absorbance of these coatings. The total surface coverage fraction is much below the percolation threshold, the interparticle separations are too large for any direct conduction or tunneling charge transfer, and the coatings are insulating.

The convective assembly process, which drives particles into the drying liquid film, can create discontinuous "stripe"-like coatings when the meniscus withdrawal speed exceeds the rate of particle influx required to form a continuous aggregated coating.[26] These stripes of aggregated nanoparticles extend the length of the meniscus, can be several hundred micrometers wide, and are highly aggregated. At faster deposition speeds, the packing density within the "stripes" does not change appreciably, but the spacing between them increases.[26] The effective concentration of particles per area of the thin film decreases, which corresponds to the observed decrease in coating absorbance spectra (without significant spectral shifts). As the stripes become thinner and get farther apart, the number of percolated networks available for electrical conductance decreases.

The most interesting electric behavior was observed with coatings deposited at intermediate deposition speeds (2 μm/s < $v_w \le 8$ μm/s). The resistance rapidly increased to 2480 $\pm$ 1460 Ω at 2.1 μm/s and jumped to 106 400 $\pm$ 25 900 Ω at 4.2 μm/s. This suggests that the structure of these films approached the percolation threshold, where the discontinu-

(47) Hohlfeld, J.; Muller, J. G.; Wellershoff, S. S.; Matthias, E. *Appl. Phys. B* **1997**, *64*, 387−390.

(48) Gao, W.; Sammes, N. M. *An Introduction to Electronic and Ionic Materials*; World Scientific Publishing Co.: River Edge, NJ, 2000.
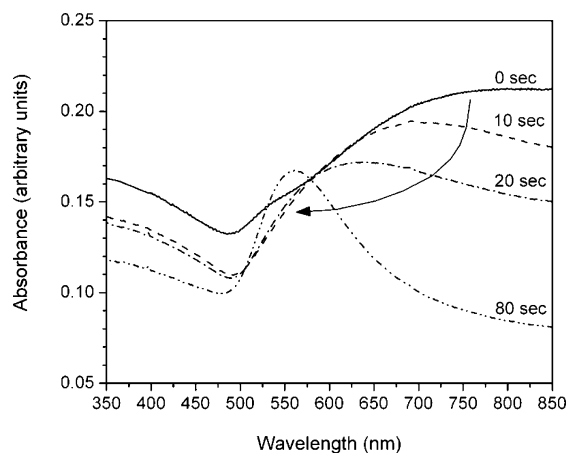(49) Sondheimer, E. H. *Adv. Phys.* **1952**, *1*, 1−42.

Figure 3. Absorbance spectra of gold coatings deposited at $v_w = 4.2$ μm/s after different durations of flame annealing.

ous aggregate microstructures quickly become insulating.[9] The plunge in electrical conductance correlates well with the optical absorbance data, as it occurred at the end of the rapid decrease of the optical density of the substrate (Figure 2). The conductivities for these coatings were measured with some instability and fluctuations during the measurements. At threshold voltages that varied between 3 and 12 V, the measured current would jump rapidly 2- to 5-fold. The increased conductance would then hold out during the voltage ramp down to 0 V. Such jumps or nonohmic "switching" effects are intrinsically characteristic of any type of metallic nanoparticle films having structures that are near the percolation region.[9,31] The nonuniform response of these films can be attributed to the limited and variable conduction pathways between the nanoparticles. Cycling and consistency studies were not performed in this study. As the experiments were performed at ambient conditions, and the coatings themselves were formed from an evaporating aqueous suspension, it is possible that adsorbed exogenics or traces of water in the nanoparticle matrix are also responsible for the switching effects.[7,31]

Effect of Annealing. The annealing by flash-heating led to a rapid and strong blue shift in the optical spectra of the coatings. The evolution of coating UV−vis absorbance spectra with time (of flame exposure) is shown in Figure 3. Several minutes of flame exposure were sufficient to shift the plasmon absorbance band from ∼800 nm to a final wavelength of ∼565 nm (Figures 3 and 4a). This change in the spectra upon heating was accompanied by a change in the macroscopic color of the films in transmitted illumination from bluish to purple and finally to reddish (while remaining semitransparent at all stages, see also Figure 1b). Similar color transitions upon heating have been reported for evaporated, discontinuous silver and gold films.[8,50] Plasmon peak blue shifts due to heating have previously been reported in thin polymer films with embedded silver nanoparticles,[9] and have long been known to occur for gold "ruby" glasses.[51] No further blue shifting was observed for additional annealing times greater than 2−3 min. During this shift the SPR
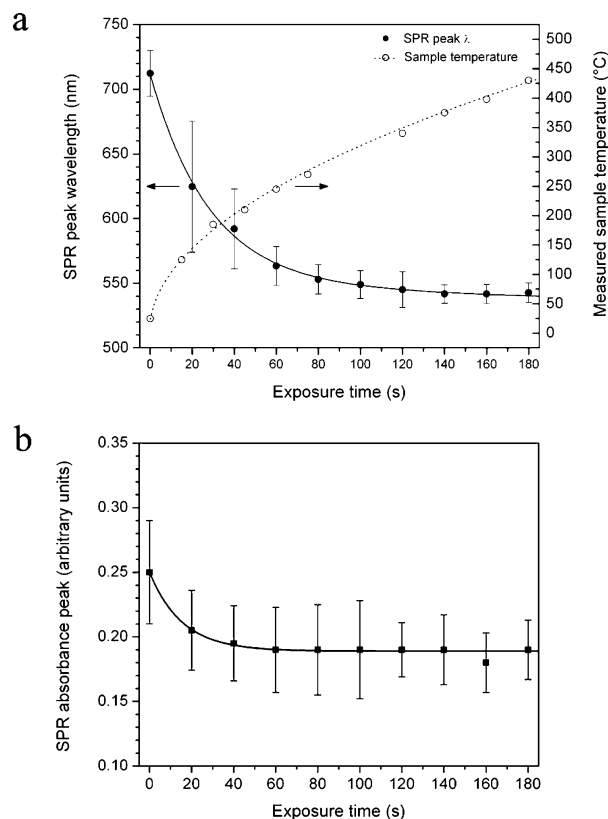

Figure 4. (a) Evolution of the SPR peak wavelength compared to the approximate temperature as a function of exposure time. (b) SPR absorbance peak for increasing heating durations. The lines are to guide the eye.

absorbance band became much narrower, and the overall absorbance of the film decreased by ca. 20% (Figure 4b).

The change in coating coloration and the spectral blue shift of the SPR absorbance to lower wavelengths (∼565 nm) after heating indicate a decrease in the average domain size of the metal microstructure. On the basis of the SPR at ∼565 nm, the heated gold nanocoatings behaved as if they were composed of isolated particle-like objects about 90 nm in size.[52] Such conclusions about the coating microstructure correlate with the changes observed in electrical conductance of the nanocoatings after annealing. Flame annealing for less than 20 s of coatings deposited at $v_w \leq 2.1$ μm/s increased their conductance by up to an order of magnitude, similar to the behavior of vacuum-deposited discontinuous metallic films.[9] All coatings became insulating ($R_S > 2 \times 10^9$ Ω) after being flame-heated for longer than 30 s, which coincides with the amount of heat exposure time it took to strongly blue shift the SPR absorbance of the coatings.

The UV−vis spectra and electrical conductance data imply that short annealing durations sintered neighboring nanoparticles and improved electrical connections, while longer durations of annealing ruptured the coating into an electrically insulating, discontinuous film of isolated nanoscale particles. The changes in the absorbance spectra and electrical conductance after thermal annealing could be directly correlated to the coating microstructure observed by scanning electron microscopy (SEM). The untreated gold nanocoatings exhibited a uniform, multilayer aggregated nanoparticle

(50) Kennerly, S. W.; Little, J. W.; Warmack, R. J.; Ferrell, T. L. *Phys. Rev. B* **1984**, *29*, 2926−2929.
(51) Eitel, W. *Physical Chemistry of Silicates*; University of Chicago Press: Chicago, 1954.

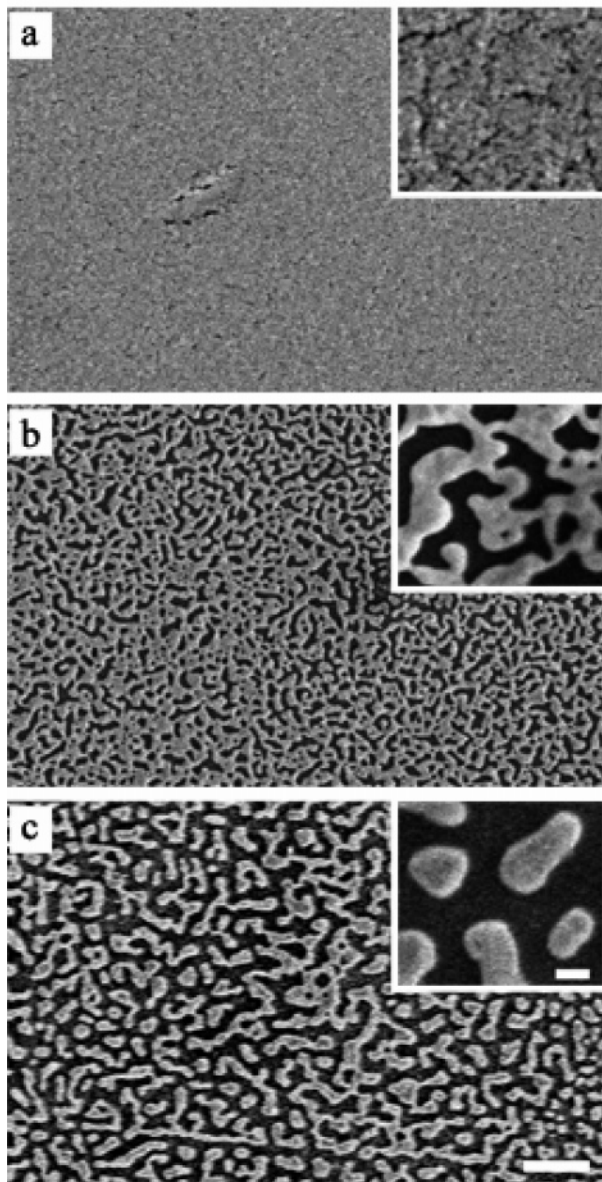(52) Link, S.; El-Sayed, M. A. *J. Phys. Chem. B* **1999**, *103*, 421−4217.

Figure 5. Scanning electron micrographs of gold nanocoatings deposited at $v_w = 2.1$ um/s, heated for increasing time durations: (a) initial aggregated nanoparticle multilayers as-deposited (no heat treatment); (b) flame-annealed for 20 s; and (c) flame-annealed for 2 min. The insets are high magnification images; large image scale bar = 1 μm, inset scale bar = 100 nm.

structure (Figure 5a). Short durations of ~10−20 s of flame-heating were sufficient to fuse the microstructure by sintering the particles together (Figure 5b). The elimination of the intraparticle grain boundaries and interparticle point contacts is the likely reason for the reduced resistance imparted by the short-term heating. The same structure as that shown in Figure 5b could be achieved by one minute or more of microwaving.

Flame annealing for durations in excess of 30 s changed the coating morphology from highly aggregated nanoparticles to discrete "droplets" or islands approximately 50−200 nm in size (Figure 5c). This change in the microstructure, from thin films of aggregated gold nanoparticles to discrete, discontinuous nanosized "droplets", is irreversible. The observed size of the consolidated nanoparticle islands corresponds well to optical spectra data, where ~90 nm effective

domain size was deduced from the final SPR position of 565 nm.[52] The surface coverage fraction of the gold coating, *f*, decreased as the coatings were heated for longer times. This effect is clearly seen in Figure 5, as the visible fraction of the glass substrate (black) decreased from ~0.8 to ~0.6 for coatings subjected to brief heating (10−30 s) and to ~0.4 for coatings subjected to long heating (*t* > 2 min). These observations help to explain the decrease in the measured absorbance magnitude after heating shown in Figure 4b. This postheating effect is analogous to the reduced absorbance intensity seen for unheated coatings deposited at more rapid deposition speeds (Figure 2).

In addition to the decrease in surface coverage fraction upon heating, the local nanostructure became significantly smoother and the porosity decreased as the particles fused together upon heating, reducing the interstitial void space between particles (see insets of Figure 5). This microstructural rearrangement is also likely to change the extinction coefficient of the coatings by the effective change in average particle size. Additionally, the poor wetting of the gold on the glass may induce a beading effect that raises the effective height of the gold droplets from their previous aggregate film thickness. BET porosimetry could arguably help decouple these factors by measuring the change in the total available pore volume before and after heating. BET, however, may not be reliable due to the sensitivity of the coatings to temperatures exceeding several hundred degrees centigrade (required for accurate degassing and calibration). In contrast to flame heating, even at long exposure times, microwave radiation never effectively disrupted the coating microstructure beyond that of the image shown in Figure 5b. Thus, microwave treatment provided only enough energy to sinter the aggregated particles together, which could be because the microwave-transparent substrates acted as a heat sink.

The results prove that the heat treatment allows easy control of the nanocoating structure, which is directly correlated to the resulting change in their optical and electric properties. The data complement literature results obtained with gold nanostructures made by alternative methods. In previously reported systems of sputtered Au or Ag nanoparticles embedded in plasma polymer films (instead of an air matrix on a glass substrate), cross-sectional TEM has shown that a decrease in filling fraction has been accompanied by growth of the nanoparticles in the vertical dimension perpendicular to the substrate.[9]

Coating Adhesion and Cohesion. The adhesive and cohesive properties of the nanoparticle coatings are of interest in view of their stability and durability in practical applications. Pure gold adheres poorly to glass surfaces, which necessitates the deposition of an underlying chromium layer in vacuum evaporation processes. The commonly used sterically protected gold nanoparticles do not adhere well to each other or to most substrates, and after deposition they are readily redispersed by sonication in suitable organic solvents. Unprotected gold nanoparticles adhere well to each other because of the strong van der Waals attraction between metals, and the gold−glass adhesion is stronger than the adhesion between sterically protected nanoparticles and glass. We believe that this increased cohesion and adhesion of
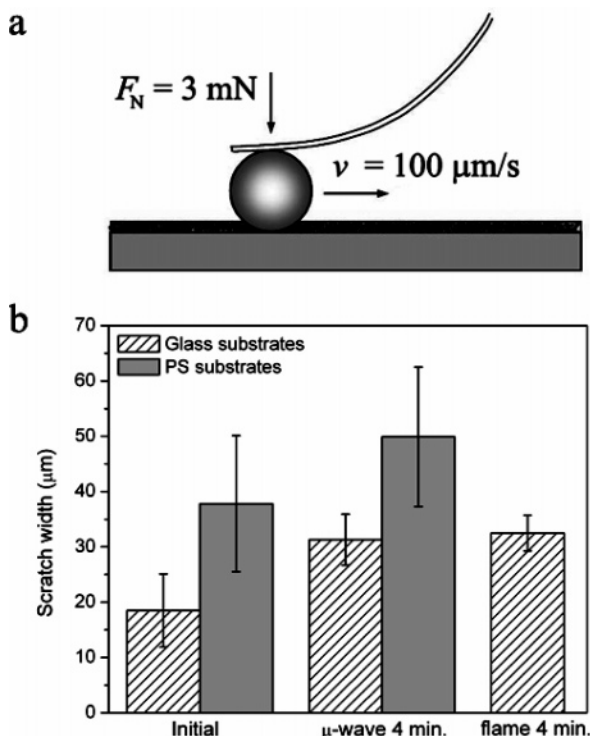
a

b

Figure 6. Evaluation of coating adhesion before and after heating by scratch testing: (a) experimental parameters; and (b) comparison of scratch widths for unheated, flame-annealed, and microwaved coatings.

"naked" particles, was the major reason the as-deposited films would not redisperse when immersed in water or acetone (and subjected to sonication).

The nanocoatings could be removed reatively easily by mechanical means. The custom designed "scratch" test revealed the poor adhesion of the unmodified nanocoatings to the substrates (the parameters of the scratch test are shown in Figure 6a). In every sample, the films in the path of the ball were removed, leaving no gold behind. Scratch width universally increased from the unmodified control coatings to the flash-heated coatings (Figure 6b). The same effect was observed when the substrates were PS microscope slides heated by microwaving, however, the widths of the scratches on the PS slides were consistently wider than those on glass (Figure 6b). Thus, within the precision of this test, neither thermal nor microwave heating improved the (generally weak) gold-substrate *adhesion*. The increase in scratch width upon heating, however, suggests that heat treatment improved the *cohesion* of the gold coating. The stronger cohesion results from the nanoparticles becoming fused together in the region of the interparticle contacts, and then being removed collectively by the "scratching" ball. This was corroborated by the SEM evidence showing fused nanoparticles in the heat-treated coatings, and discrete aggregated nanoparticles in the unmodified coatings (Figure 5). Thus, while neither heating technique measurably improved the gold coating adhesion, they both yielded a stronger, more cohesive coating.

In general, the convective deposition technique has several key parameters for adjusting the coating coverage: the meniscus withdrawal speed, v_w, the concentration of the particles, and the rate of the carrier solvent evaporation.[26] Gold sol concentrations below 2–3 wt % are too low to yield

complete uniform coverage and are not of concern in this study. The rate of solvent evaporation was previously shown to have little effect in the range of deposition speeds studied (0.5–20 μm/s).[26] Thus, v_w remains the most potent variable for controlling the coating properties and can be adjusted easily to deposit films of desired thickness. The coating thickness and the surface concentration of nanoparticles directly affect the absorbance intensity and electrical conductivity (see Figure 2b).

The degree of particle aggregation or the average gold domain size cannot be controlled by the deposition process (see Figures 2a and 5a). There were no adsorbed polymer layers on the substrate, nor were there any steric ligands on the particles to prevent aggregation when the solvent is removed. The SEM, conductance, and UV–vis spectrophotometric data prove that the nanoparticles are in direct electric contact. The convective assembly process drives the particles together into an aggregated film that has a percolated structure at the lower rates of meniscus withdrawal, and an increasingly discontinuous, insulating structure at higher withdrawal rates. Post-deposition heat treatment provided a convenient means to tune the nanocoatings microstructure from aggregated gold domains larger than micrometers to discrete, discontinuous ~50–200 nm gold islands (Figure 5c). These heat-induced structural changes are irreversible, but can be instituted incrementally by varying the annealing time. The optical properties, which are shown to directly depend on the coating microstructure, can be efficiently tuned. This method is the first to permit deposition of multilayers from unfunctionalized nanoparticles. The increased number of layers should provide more electronic conductance pathways and improved film properties. Gold nanocoatings with dense, near percolated structures could make temperature-sensitive devices (e.g., fuses) or other sensors based on their optical or electrical responses to external stimuli.

Conclusions

We report how films formed from unprotected metallic nanoparticles were deposited directly from water suspensions. Such multilayer films cannot be fabricated by the vacuum deposition and electrostatic or chemical self-assembly methods used to date. Convective assembly is shown to be an efficient technique for controllable deposition of films from nanoparticles in suspension. It is simple, inexpensive, and easily scalable, and works on virtually any type of substrate without need for preliminary chemical functionalization. The method allows facile tuning of the thickness of the deposited material from submonolayers to thick multilayers. While the nanoparticles in these films are not ordered *per se*, the structure of the coating could be controllably varied above and below the percolation threshold by either adjusting the deposition speed or annealing the coatings for brief durations after deposition at temperatures well below the bulk gold melting point. The coating plasmon resonance could be tuned from 800 to 565 nm and the electrical conductivities ranged from 2000 Ω^{-1} cm^{-1} to less than 10^{-5} Ω^{-1} cm^{-1}. Controlling and tuning the optical and electric properties of these nanocoatings may allow their use in conductive and semi-

transparent films, heat fuses, or planar catalytic substrates. Additional chemical functionalization of the particles, before or after film assembly, could lead to applications such as elements with nonlinear electronic or photonic properties, substrates for quantum electronic devices, catalytic surfaces, and chemical/bio sensors.